Thesis for the Degree of Master of Science (20p)

Model of Chemotaxis with Limited Cell Density

Vivi Andasari

CHALMERS | GÖTEBORG UNIVERSITY

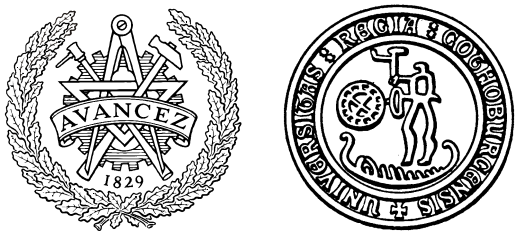

Department of Mathematics
Chalmers University of Technology and Göteborg University
SE – 412 96 Göteborg, Sweden
Göteborg, May 2004

Acknowledgements

This thesis is submitted as part of the requirements in the International Master's Programme in Engineering Mathematics at the Department of Mathematics, Chalmers University of Technology.

I would like to thank to those that have supported me during my work:

- Bernt Wennberg, as my supervisor,
- Stig Larsson, for always being so helpful,
- My beloved family in Indonesia,
- Ivar Gustafsson and Ann-Britt Karlsson, director and coordinator for the International Master's Programme of Department of Mathematics, thank you for the wonderful activities of the programme,
- Anders Logg, for the discussions and numerous suggestions,
- My marvellous Indonesian companions,
- Engineering Mathematics classmates of year 2002,
- to STINT (Stiftelsen för internationalisering av högre utbildning och forskning) for financially supporting my studies in Sweden.
- and to all of my friends in the Department of Mathematics of Chalmers and in Göteborg.

Göteborg, May 19th 2004

Abstract

There is an obvious need to study how cells react in their environment. Many cells respond to the presence of chemical substances. When detecting the chemicals, cells make particular movements by which they can develop, heal wounds, protect against invaders, create blood vessels, etc. Mathematical models of cell behaviour and movement have been studied in order to understand these complex processes. One that we discuss here is the movement of cells *up* gradient in the presence of chemical attractants, renowned as *chemotaxis*. We derive the widely used model for chemotaxis, the Keller-Segel model which is a system of Reaction-Diffusion-Convection equations. The model has been derived from the conservation laws using Fickian-assumption, and we also perform stability analysis of the model. Solutions of the equations may blow up in finite time in 2 dimensional space. We study a modified model using volume-filling mechanism with Allee effect for cell density and saturating rate mechanism with Michaelis-Menten kinetics for chemical attractant density. Both are applied to modify the Keller-Segel equations into a model that can be used to prevent blow up. Numerical simulations are accomplished using the Finite Element Method.

Contents

List of Figures

Chapter 1

Introduction

The nature we live in is full with amazing wonders and it continually astonishes us with its infinite variation that attracts scientists to dissect what lies behind the phenomena. For instance, the nature has immensely big variety of "invisible", "inaudible" smells upon which all living organisms, from single cell organisms such as bacteria and amoebae to multi cellular organisms such as insects and mammals, depend for their lives through chemical communications that occur upon the completion of three essential steps: (a) the release of a chemical signal, (b) the transmission of that signal through the environment, and (c) reception of signal by another individual (28). The simplest important exploitation of chemical signal release is a directed movement it can generate in a population of organisms. The knowledge about chemically directed movement is renowned as *chemotaxis*, that is the ability to sense the direction of external chemical signals or sources and to respond by polarizing and migrating towards chemical attractants or away from chemical repellants.

Chemotaxis is crucial for proper functioning of multi cellular organisms as well as single cell organisms. As an example in (24), the female silk moth *Bombyx mori* exudes a pheromone called bombykol to attract male moth that detects the bombykol by its remarkably efficient antenna filter that measures the bombykol concentration, the male moth will move in the direction of increasing concentration. Another example of chemotaxis is the use of smell for communication and predation by deep sea fish. Chemotaxis in single cell organisms in biological processes is significant for many purposes.

In chapter 2, we outline some applications of chemotaxis in medical and biomedical disciplines. Then we discuss biological background cellular slime mold amoebae *Dictyostelium discoideum* including its life cycle and its chemical attractant, which have aroused the interest of many scientists. Here we also give a brief explanation about the values of mathematical modelling in biology, where the studies of chemotaxis have been categorized into stochastic approach and deterministic approach.

The first mathematical model of chemotaxis was introduced by C.S. Patlak in 1953. Evelyn Fox Keller and Lee A. Segel then boosted the model by their work in 1970. Chapter 3 entails derivation of Patlak-Keller-Segel or Keller-Segel model from Fick's law with one chemical attractant. Steady state and linear stability analysis of the Keller-Segel model are performed, as well as theory of blow up possibility of the Keller-Segel model. Later we discuss a modification of the Keller-Segel model that can prevent blow up of solutions by incorporating the Allee effect in the volume-filling mechanism to prevent cells overcrowding and Michaelis-Menten kinetics of a saturation mechanism in the production of chemical attractant. Stability analysis for the modified model is also performed here.

The foregoing studies of chemotaxis and simulation of chemotaxis using the Finite Element Method provide one of the motivations for our work. As a numerical tool that is usually used for Partial Differential Equations, we employ the Finite Element Method as our means in numerical simulations, given in Chapter 4. Chapter 5 discusses reviews of chemotaxis from previous studies and researches.

Chapter 2

Biology and Mathematical Values of Chemotaxis

2.1 Applications of Chemotaxis

The focus of our discussion is chemotaxis in biological processes of molecular level. In vitro experiments have shown that chemotaxis allows single cell organisms, or cells, to detect chemicals with exquisite sensitivity. Some chemotactic cells can sense chemical gradients that differ by only a few percent from cell's front to its back. It has been discovered that a cell is able to discriminate between a relative chemical attractant concentration of 100 at its front and 99 at its back, the threshold spatial gradient of chemical attractant between ends of a cell is around 1% of the mean concentration around the cell. This was experimentally studied by Peter van Haastert in his article (35) and references therein.

By sensing its environment and then moving in chemotactically *up* gradient towards their attractants, cells can develop, heal wounds, protect against invaders, and create blood vessels.

Chemotaxis has been shown to play an integral role in cell guidance and tissue organisation during embryonic growth. It is also a major component of inflammatory, mammalian reproductive systems (spermatozoa), development of the nervous system which crucially depends on the detection and response to a group of chemical signals by the tip of the growing nerve cells (growth cone), and tumor growth where the stimulation of new blood vessel growth ("angiogenesis") mediated by chemotaxis is an indicator of increased malignancy (16).

Chemotaxis and signal transduction by chemical attractant receptors also play a key role in arthritis, asthma, lymphocyte trafficking, and in axon guidance.

In formation of patterns on animal skin, a generalized Turing model with chemotaxis was developed by Painter et. al. (31) to account for cell growth and movement. Chemotaxis in response to chemical gradients leads to aggregation of one type of pigment cell into a striped spatial pattern. Most of the original chemotactic models considered interactions between one cell type and one chemical attractant, as we are going to discuss in this thesis. However, models with two types of chemicals, an attractant and a repellent, have been discussed, such as that by Painter et. al. (31) and Luca et. al. (5).

2.2 Dictyostelium discoideum

The slime mold amoebae of type *Dictyostelium discoideum* or *D. discoideum* for short, is a unicellular eukaryote, and belongs to the kingdom of Protista. It was discovered by K.B. Raper in 1935 (18).

This species has been the subject of some researches in cell biology. *D. discoideum* offers numerous research advantages, with primary benefit that its genetic system is easily amenable to experimentation without accompanied by cell divisions. It uses the signaling pathway for finding food, for intercellular communication, and for starting its differentiation from free-floating amoebae to a multicellular organism. It can also be grown in large quantities.

D. discoideum is widely used for studying fundamental cellular processes, such as chemotaxis, cytokinesis, motility, phagocytosis, signal transduction, and aspects of development such as cell sorting, pattern formation, and cell-type determination. Many of these cellular behaviors and biochemical mechanisms are either absent or less accessible in other model organisms.

Segel (34) and Lin (21) gave detailed information in their books the following facts about chemotaxis in *D. discoideum*.

2.2.1 Life Cycle of Slime Mold D. discoideum

The slime mold amoebae can be found throughout the world in their natural habitat, soil. One can begin a description of the life cycle of the amoebae at

the spore stage, where each amoeba is dormant within protective covering. This phase is also known as the vegetative stage. When the conditions are favorable the spore will germinate, and an amoeba will emerge from its protective casing. Of the order of 10 micrometers (10^{-3} cm) across, the amoebae are rather shapeless one-celled organisms that move by extending contractile portions of themselves (pseudopods).

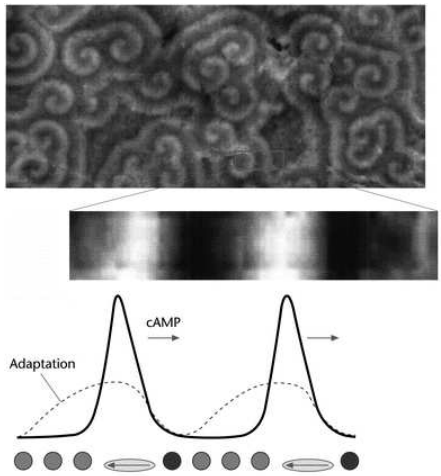

Figure 2.1: Spiral waves of cells movement in response to cAMP propagation. Courtesy of Nature Encyclopedia of Life Sciences (36)

As an important element of the food chain on earth, the amoebae feed on bacteria by engulfing them. If food is plentiful, the amoebae continually feed and multiply by mitosis (dividing in two) (more or less in every **three hours** according to Segel (34)). If the food supply becomes exhausted, the amoebae move about randomly for several hours (eight hours according to Segel (34)), then an initially uniform amoebae distribution develops what appear to be centers of organization called *aggregation sites*. Amoebae are attracted to these loci and move towards them, often in a pulsating, wavelike manner. During this period, the disappearance of the food supply triggers certain changes in the amoebae whose details are not known up to now. Contacts begin to form between neighbors, and streams of amoebae converge on a single site, eventually forming a shapeless multicellular slug that wanders as a unit towards light and more humid conditions.

Some formerly free living amoebae retain their cell walls within the slug. Then the slug stops and for several hours goes through a period of "purposeful" internal motion and change. At the end of this time, the slug has transformed itself into two cell types, stalk cells and spore cells which both build a system of slender stalk bearing a roundish container of spores at top of it. Thus the cycle is completed.

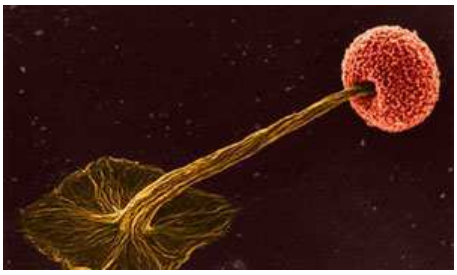

Figure 2.2: Delicated stalk body, after completing a cycle. From The Scientist magazine online

Furthermore, in order to provide rigid structural basis for holding the container of spores, the stalk cells harden and eventually die. As a result of this self-sacrifice, the spore cells are provided with an opportunity to survive the harsh conditions, to be dispersed by air currents, and to propagate the species into more favorable environments. If a spore is transported to a place that is favorable for germination, the whole cycle will begin again.

2.2.2 The Role of cAMP

The aggregation of the *D. discoideum* takes place because the amoebae are attracted to a relatively high concentrations of a chemical that they themselves secrete. The attractant has been identified as cyclic adenosine 3',5'-monophosphate, or called *cyclic* AMP or simply cAMP. It has also been shown that the cells secrete the enzyme **phosphodiesterase** that catalyzes the breaking of a bond in cAMP, turning it into 5'-AMP which is not a chemoattractant for the amoebae.

The discovery that cAMP plays a major role in *D. discoideum* gave great impetus to the study of this organism, for cAMP also has a major function in mammalian physiology as the "universal second messenger" of hormone action.

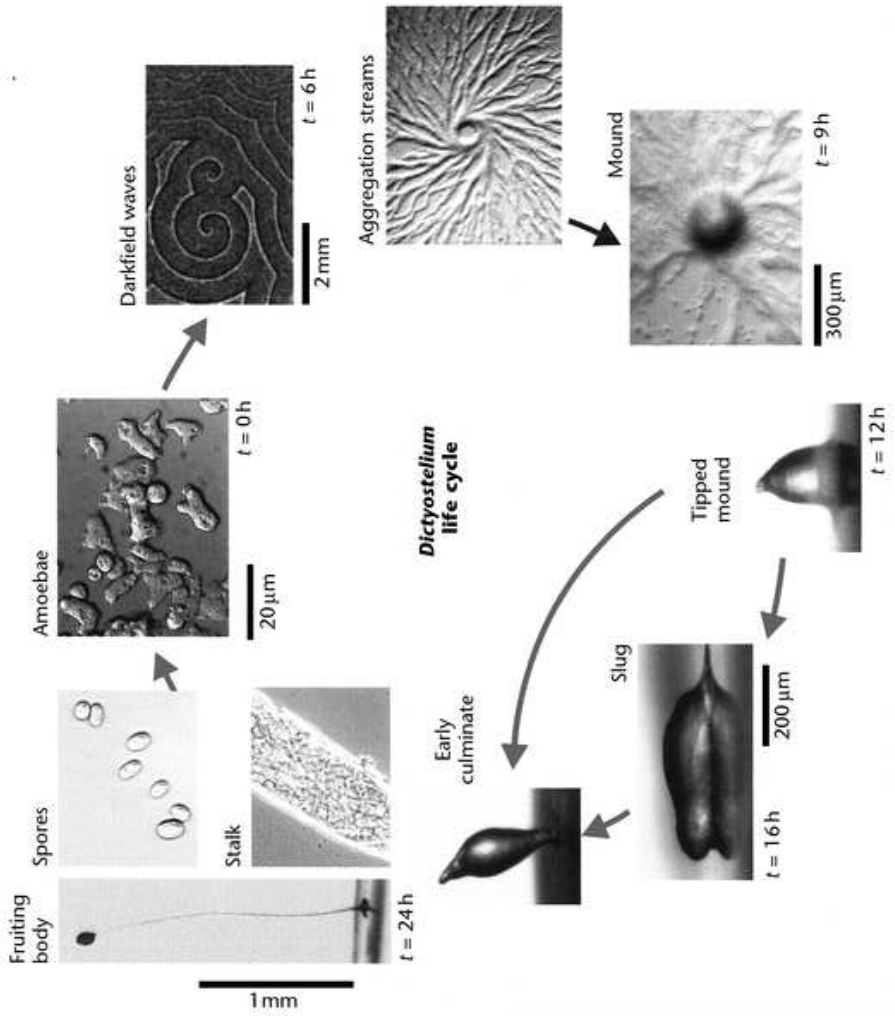

Figure 2.3: Life cycle of Dictyostelium discoideum, in a clockwise order starting at the top. Courtesy of Nature Encyclopedia of Life Sciences (36)

E.W. Sutherland was awarded the Nobel prize for medicine in 1971 for his work in elucidating some of the roles of cAMP.

In a typical aggregation pattern in *D. discoideum*, individual amoebae move steadily towards the aggregation center for about **a minute and a half**, and then make no further progress for a period of approximately **three to eight minutes**. The steps of aggregation occur in sequence: First the cells nearest the center step inward, then an adjacent ring of cells farther out steps in, then the next outward ring, and so forth. Thus, aggregation takes place in pulses, or cAMP is released during cell aggregation in a pulsatile manner by the aggregation center. Cells in the neighborhood of the center detect cAMP, react chemotactically, and excrete cAMP themselves by which the cAMP signal is relayed.

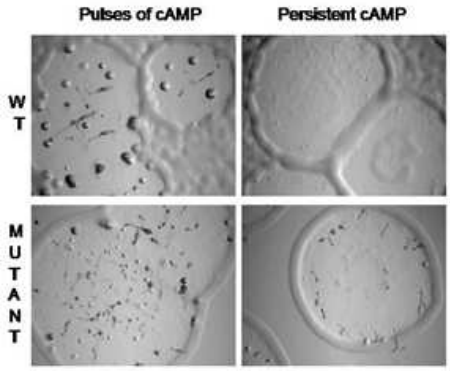

Figure 2.4: cAMP pulses, taken from http://www.hopkinsmedicine.org/cellbio/profiles/

2.3 The Value of Mathematical Models

The first breakthrough in modern mathematical biology was started when Lotka (1924) and Volterra (1926) established their works on the expression of predator-prey and competing species relations in terms of simultaneous nonlinear differential equations. Since then mathematicians and biologists have attempted to study and analyze the dynamics of ecosystems as well as to make the quantitative prediction of phenomena in nature into mathematical models.

Mathematical models can be broadly categorized into two types, as quoted by Okubo (28). One may be referred to as "educational", and the other as

"practical" in nature. Educational models are based on a small number of simple assumptions and are analitically tractable. The real virtue of these models lies in the fact that they provide a process for gaining insight, expressing ideas, and eventually extending to more complex models. Practical models are based on realistic assumptions and thus involve the parameterization of interrelationships of large numbers of variables, and often the formulation of numerous equations containing numerous parameters is required. In such cases analytical treatment becomes impossible, and one must rely on computer calculations for numerical approximations.

Mathematical models can also be delineated into deterministic models and stochastic nature. Educational models often employ deterministic methods, while practical models tend to be stochastic in approach. Many biological structures and processes are intrinsically stochastic. However, a greater portion of the individuals involved in a process may be said to follow a single deterministic path on the average.

In summary, the phenomenon of chemotaxis as the topic of our discussion has been mathematically studied and divided in 2 approaches as follow:

- Stochastic processes for the position and moving direction of each individual, and
- Partial Differential Equations for the density and the mean flux of whole population (deterministic model)

In this thesis, emphasis has been placed on continuum-based model used in deterministic approach.

Chapter 3

Mathematical Model for Chemotaxis

3.1 Formulation of Keller-Segel Model

The motions, migrations, and redistributions of cell populations are of some interest for scientists because the cell populations are rarely distributed evenly over a featureless environment. On individual level, the movement might result from amoeboid streaming. On collective level it is often appropriate to make a *continuum* assumption, that is, to depict discrete cells or organisms by continuous density distributions. This assumption leads to Partial Differential Equation (PDE) models that constructed a model introduced by Patlak, Keller, and Segel, known as the Keller-Segel model, for molecular diffusion, convection, or attraction that we discuss in this section.

Most of PDEs are ultimately based on the conservation law and its various forms. Some recent literature are good start to understand the implementation of conservation laws in biological settings, such as books by Edelstein-Keshet (6), J.D. Murray (24), Okubo (28), and Fall et. al. (7).

We start deriving the Keller-Segel model by letting S be an arbitrary surface enclosing a volume V. From the general conservation equation, the rate of change of the amount of material u in V is equal to the rate of flow of material across S into V plus the material created in V. Thus

$$\frac{\partial}{\partial t}\int_V u\,dv = -\int_S \mathrm{J}\cdot n\,ds + \int_V f\,dv \tag{3.1}$$

where J is the flux of material and f represents the source of material.

By the Divergence theorem

$$\int_S \mathrm{J} \cdot n \, ds = \int_V \nabla \cdot \mathrm{J} \, dv \tag{3.2}$$

and assuming that the function u is continuous, the first equation becomes (rewrite $\frac{\partial u}{\partial t}$ into u_t)

$$\int_V [u_t + \nabla \cdot \mathrm{J} - f] \, dv = 0 \tag{3.3}$$

Since the volume V is arbitrary the integrand must be zero and the *conservation equation* for u then reads

$$u_t + \nabla \cdot \mathrm{J} = f \tag{3.4}$$

This equation holds for a general flux transport J whether by diffusion or by some other processes.

If we consider the Fick's law as the process of diffusion,

$$\mathrm{J} = -D\nabla u \tag{3.5}$$

then equation (3.4) becomes

$$u_t = \nabla \cdot (D\nabla u) + f \tag{3.6}$$

where D may be a constant or depend on space, time, or even on u.

Applying the formulations to chemotaxis, let us suppose u represents the cell density, and v a chemical attractant. Biological experiments show that the presence of a gradient in attractant gives rise to a movement of the cells in *up* gradient. The flux of cells will increase with the number of cells present. There is another flux that plays significant role in the process, that is the chemotactic flux

$$\mathrm{J} = \chi u \nabla v \tag{3.7}$$

where χ is chemotactic coefficient. Analysis of χ in various forms has been carried out, such as by Katharina Post (33), Painter and Hillen (15), and Schaaf (see reference in (5)). The most used is χ as a positive constant. Now the flux has contribution from diffusion flux equation (3.5) and chemotaxis flux of equation (3.7)

$$\mathrm{J} = \mathrm{J}_{\text{diffusion}} + \mathrm{J}_{\text{chemotaxis}}$$

Subtituting equations (3.7) and (3.5) into (3.4) yields

$$u_t = \nabla \cdot D_1 \nabla u - \nabla \cdot \chi u \nabla v + f(u, v) \tag{3.8}$$

where D_1 is the diffusion coefficient of the cells. Now the term $f(u, v)$ is a function of u and v and it represents cell proliferation and death.

The chemical attractant v also diffuses and is produced by the cells themselves. For one chemical attractant, the equation for v can typically be in the from

$$v_t = \nabla \cdot D_2 \nabla v + g(u, v) \tag{3.9}$$

The first term in the right hand side expresses the diffusion of the attractant with diffusion coefficient D_2, and the second term $g(u, v)$ is kinetics or source term that represents production and/or degradation of attractant.

To give a minimal model for aggregation phase, Keller and Segel made a number of simplifying assumptions (6):

1. Individual cells undergo a combination of random motion and chemotaxis towards chemical attractant.

2. Cells neither die nor divide during aggregation.

3. The attractant is produced at a constant rate by each cell.

4. The rate of degradation of attractant depends linearly on its concentration.

5. The attractant diffuses passively over the aggregation field.

Using these assumptions, the cell proliferation and death term $f(u, v)$ in equation (3.8) is set to be zero and the term $g(u, v)$ in equation (3.9) is expanded to $\alpha u - \beta v$ where α and β are the rates of chemical production and degradation, respectively, they are assumed to be positive constants. Taking D_1, D_2 and χ also to be positive constants, thus the parabolic quasi-linear strongly coupled system of Keller-Segel is

$$u_t = D_1 \nabla^2 u - \nabla \cdot \chi u \nabla v \quad ; \quad x \in \Omega, \quad t > 0 \tag{3.10}$$

$$v_t = D_2 \nabla^2 v + \alpha u - \beta v \quad ; \quad x \in \Omega, \quad t > 0 \tag{3.11}$$

Equation (3.10) and (3.11) are to be completed with initial and boundary conditions. If we assume that the population to stay constant during chemotactic aggregation, then it is natural to impose no-flux boundary conditions

$$\frac{\partial u}{\partial n} = \frac{\partial v}{\partial n} = 0 \quad \text{for } x \in \partial\Omega, \quad t > 0$$

and the initial data as smooth non-negative functions

$$u(x,0) = u_0(x), \quad v(x,0) = v_0(x) \quad \text{for } x \in \Omega$$

This gives two linear equations when it is seen as separate, but the strong coupling term $\nabla \cdot \chi u \nabla v$ makes the system strongly nonlinear. And this term describes aggregation directed towards the center of aggregation with velocity proportional to ∇v. In the absence of this term cells move in random way.

3.2 Analysis of the Keller-Segel Model

3.2.1 Homogeneous Steady States

Let us now study the homogeneous steady state of the classical Keller-Segel system. Homogeneous steady state of a PDE model is a solution that is constant in space and in time, and such solutions must satisfy the following

$$u(x,t) = \bar{u}, \qquad v(x,t) = \bar{v} \tag{3.12}$$

where

$$\frac{\partial \bar{u}}{\partial t} = \frac{\partial \bar{v}}{\partial t} = 0 \tag{3.13}$$

$$\frac{\partial \bar{u}}{\partial x} = \frac{\partial \bar{v}}{\partial x} = 0 \tag{3.14}$$

Substituting these equations into (3.10) and (3.11) gives

$$\begin{aligned} 0 &= 0\,, \\ 0 &= 0 + \alpha\bar{u} - \beta\bar{v} \end{aligned} \tag{3.15}$$

Then it must follow that

$$\alpha\bar{u} = \beta\bar{v} \tag{3.16}$$

This means that in the uniform state the secretion rate of attractant must be exactly balanced by the decay rate.

3.2.2 Stability Analysis

A reaction-diffusion system exhibits diffusion-driven instability, sometimes called *Turing instability*, if the homogeneous steady state is stable to small perturbations in the absence of diffusion but unstable to small spatial perturbations when diffusion is present (25). The main process driving the spatially inhomogeneous instability is diffusion: the mechanism determines the spatial pattern that evolves.

In determining the necessary and sufficient conditions for diffusion-driven instability of the steady state and the initiation for the general system, or biologically, to determine whether aggregation of cells is likely to begin, we look at the spatially inhomogeneous perturbations and then we explore whether the perturbations are amplified or attenuated.

If an amplification occurs, then a situation close to the spatially uniform steady state will destabilize, leading to some new state in which spatial variations predominate, and even there could possibly exist oscillating solutions. This process of destabilization is identified as the onset of aggregation and is presumed to happen because of changes of the parameters D_1, D_2, χ, and α.

We perform the stability analysis in one dimension. Introduce the variables u' and v' by the definitions

$$u(x,t) = \bar{u} + u'(x,t) \tag{3.17}$$

$$v(x,t) = \bar{v} + v'(x,t) \tag{3.18}$$

where $u' = u - \bar{u}$, for example, measures departure from uniformity, it can be identified with the disturbance (perturbation) in cell density. We consider u' and v' to be small.

To obtain equations for u', we substitute (3.17) into (3.10)

$$\frac{\partial u'}{\partial t} = D_1 \frac{\partial^2 u'}{\partial x^2} - \chi \left((\bar{u} + u') \frac{\partial^2 v'}{\partial x^2} + \frac{\partial u'}{\partial x} \frac{\partial v'}{\partial x} \right) \tag{3.19}$$

This equation is nonlinear, owing to the presence of the quadratic terms $u'(\partial^2 u'/\partial x^2)$ and $(\partial u'/\partial x)(\partial v'/\partial x)$. We shall also assume that the derivative of u' and v' are small. Therefore products of two small terms should be negligible in comparison

with the other terms, which contain but a single perturbation. We thus linearize the equation by deleting all nonlinear terms and obtain

$$\frac{\partial u'}{\partial t} = D_1 \frac{\partial^2 u'}{\partial x^2} - \chi \bar{u} \frac{\partial^2 v'}{\partial x^2} \tag{3.20}$$

As for (3.11), upon substituting (3.18) we obtain

$$\frac{\partial v'}{\partial t} = D_2 \frac{\partial^2 v'}{\partial x^2} + \alpha u' - \beta v' \tag{3.21}$$

which is already linear.

We equip the perturbation equations (3.20) and (3.21) with no-flux boundary conditions and smooth initial conditions.

$$\frac{\partial u'}{\partial x} = 0 \quad \text{at} \quad x = 0,\ x = L \qquad \text{and} \quad u'(x,0) \text{ given} \tag{3.22}$$

$$\frac{\partial v'}{\partial x} = 0 \quad \text{at} \quad x = 0,\ x = L \qquad \text{and} \quad v'(x,0) \text{ given} \tag{3.23}$$

With spatial variation, u' and v' satisfy

$$u'_t = 0 \qquad v'_t = \alpha u' - \beta v' \tag{3.24}$$

Linearising about the steady state $(\bar{u}, \bar{v})$ we set

$$\mathbf{y} = \begin{pmatrix} u - \bar{u} \\ v - \bar{v} \end{pmatrix} \tag{3.25}$$

and for small $|\mathbf{y}|$, equation (3.24) becomes

$$\mathbf{y}_t = B\mathbf{y} \qquad \text{where} \quad B = \begin{pmatrix} 0 & 0 \\ \alpha & -\beta \end{pmatrix} \tag{3.26}$$

with B is regarded as the stability matrix. We now look for solutions in the form

$$\mathbf{y} \propto e^{\lambda t} \tag{3.27}$$

where λ is the eigenvalue. The steady state $\mathbf{y} = 0$ is linearly stable if $\mathbb{R}e\lambda < 0$ since in this case of perturbation $\mathbf{y} \to 0$ as $t \to \infty$.

Now we consider the full system of equations (3.20) and (3.21) and linearize about the steady state, which with equation (3.25) is $\mathbf{y} = 0$ to get

$$\mathbf{y}_t = A\nabla^2 \mathbf{y} + B\mathbf{y} \qquad A = \begin{pmatrix} D_1 & -\chi \bar{u} \\ 0 & D_2 \end{pmatrix} \tag{3.28}$$

To solve this system of equation subject to the boundary conditions, we define $\mathbf{Y}(\mathbf{r})$ to be the time-independent solution of the spatial eigenvalue problem defined by

$$\nabla^2\mathbf{Y} + k^2\mathbf{Y} = 0 \quad (\mathbf{n}\cdot\nabla)\mathbf{Y} = 0 \quad \mathbf{r} \text{ on boundaries} \tag{3.29}$$

where k is the eigenvalue. The general solution of the equation is

$$\mathbf{Y}(x) = C_1 cos(kx) + C_2 sin(kx) \tag{3.30}$$

Taking account of the boundary conditions which then force $C_2 = 0$, we get

$$\mathbf{Y} \propto cos\left(\frac{\pi n x}{L}\right) \tag{3.31}$$

where n is positive integer and we take $C_1 = 1$. The eigenvalue in this case is $k = \pi n/L$, it also represents the *wavenumber* of the perturbation and n is the mode ($2L/n$ is the wavelength in this example).

With finite domains there is a discrete set of possible wavenumber since n is an integer. Let $\mathbf{Y}_k(\mathbf{r})$ be the eigenfunction corresponding to the wavenumber k. Each eigenfunction $\mathbf{Y}_k$ satisfies no-flux boundary conditions. We now look for solutions $\mathbf{y}(\mathbf{r}, t)$ of equation (3.28) in the form

$$\mathbf{y}(\mathbf{r}, t) = \sum_k c_k\, e^{\lambda t}\, \mathbf{Y}_k(\mathbf{r}) \tag{3.32}$$

where the constants c_k are determined by a Fourier expansion of the initial conditions and λ is the eigenvalue which determines temporal growth. Substituting this into (3.28) with (3.29) and cancelling $e^{\lambda t}$, we get, for each k

$$\lambda\mathbf{Y}_k = B\mathbf{Y}_k - k^2 A\mathbf{Y}_k \tag{3.33}$$

For nontrivial solutions of $\mathbf{Y}_k$, the λ are determined by the roots of the characteristic polynomial

$$|\lambda I - B + k^2 A| = 0 \tag{3.34}$$

Inserting the elements of A and B and taking the determinant equals to zero,

$$\begin{vmatrix} \lambda + k^2 D_1 & -k\chi\bar{u} \\ -\alpha & \lambda + \beta + k^2 D_2 \end{vmatrix} = 0 \tag{3.35}$$

The resulting equation for λ is then

$$\lambda^2 + [\beta + k^2(D_1 + D_2)]\lambda + [k^4 D_1 D_2 + k^2(D_1\beta - \alpha\chi\bar{u})] \tag{3.36}$$

or, after rearranging terms, the quadratic equation in λ

$$\lambda^2 + q\lambda + \gamma = 0 \tag{3.37}$$

where

$$q = k^2(D_1 + D_2) + \beta \tag{3.38}$$

$$\gamma = k^2[D_1(D_2k^2 + \beta) - \chi\bar{u}\alpha] \tag{3.39}$$

For a system with two roots of equation to be instable, one root of real part must be negative and the other must be positive. Suppose that we take the real part of q to be positive, then it is necessary that the value of γ be negative. Therefore the condition for instability, or for aggregation to commence is determined by

$$D_1(D_2k^2 + \beta) < \chi\bar{u}\alpha \tag{3.40}$$

By $k = \pi n/L$, the inequality (3.40) implies

$$D_1\left[D_2(\frac{n\pi}{L})^2 + \beta\right] < \chi\bar{u}\alpha \tag{3.41}$$

The perturbations are characterized by their linear growth rate and wavelength $2L/n$.

From these results we can see that to satisfy instability of the inequality (3.41) it is necessary to have one or several of the following conditions:

1. Values of D_1, D_2, β, and/or n must be small
2. Values of L must be large
3. Values of $\chi, \bar{u}$, and/or α must be largee

This means that the factors elevating the onset of aggregation which leads to instability are:

1. Low random motility of the cells and low rate of degradation of attractant

2. Large chemotactic sensitivity, high secretion rate of attractant, and a high density of cells at steady state $\bar{u}$

For *D. discoideum* amoebae, it has been observed experimentally that its onset of aggregation is accompanied by an increase in chemotactic sensitivity and cAMP production. It appears that these changes bring about the condition for instability, given by inequality (3.41) that leads to aggregation. Edelstein-Keshet (6) added several other factors that also stimulate aggregation:

1. Aggregation is favored more highly in a larger domains than in smaller ones,

2. The perturbations most likely to be unstable are the perturbations with small n, as $n = 1$ or $n = 2$.

3.3 Chemotactic Collapse

Due to the quadratic nature of the convective term $\nabla \cdot \chi u \nabla v$, chemotaxis model of equations (3.10) - (3.11) is expected to have solutions exhibiting chemotactic collapse, i.e., such that the solutions may blow up in finite time for which under suitable circumstances the density of population should concentrate in a single point in finite time. In mathematical terms, this means formation of a Dirac delta-type singularity in finite time, i.e.,

$$u(x,t) \to P\,\delta(x_k) \quad \text{as } t \to T \tag{3.42}$$

for some $T < \infty$.

$$P = \int_\Omega u(x,t)\,dx = \int_\Omega u_k(x)\,dx \tag{3.43}$$

Blow up has been studied to be connected with space dimensions, which also has been shown to appear in radially symmetric solutions. In the linear case of chemotactic sensitivity as in equation (3.10) where χ is regarded as a constant, blow up in finite time never occurs in one dimension $d = 1$ (unless there is no diffusion of attractant). But blow up can always occur in d-D for $d \geq 3$. The $d = 2$ is a borderline case and there is threshold found for radially symmetric solutions. When the initial distribution exceeds this threshold, the solution may

blow up in finite time. When the initial distribution is below this threshold, then the solution exists globally.

To better understand the scenario of collapse of the radially symmetric solutions, we introduce an auxiliary mass function in a radial domain Ω,

$$M = \int_{\Omega} r^{d-1}\, u(r)\, dr \tag{3.44}$$

of the radial coordinates

$$\Delta u = \frac{1}{r}\frac{\partial}{\partial r}\, r\, \frac{\partial}{\partial r}\, u \tag{3.45}$$

Brenner and Betterton in (2) noted that if the experiment for chemotaxis takes place in a petri dish, it is *not* a quasi-two-dimensional. They explain critical dimension which is conceivable by comparing the chemotactic and diffusive fluxes in a contracting structure using cylindrical coordinates which we describe below.

From equation (3.44) we define M^{1D}, M^{2D}, and M^{3D} as mass per unit area, mass per unit length with height (cylinder), and mass contained within a sphere, respectively, in accordance to the space dimension,

$$M^{1D} = \int_{\Omega} u\, dr, \quad M^{2D} = \int_{\Omega} r\, u\, dr, \quad M^{3D} = \int_{\Omega} r^2\, u\, dr$$

If the chemotaxis is conducted on sheet with thickness l which is regarded as experiment in one dimensional with $d = 1$, the inward diffusive flux is of order

$$J_1 \sim -D_1 \frac{u}{l} \tag{3.46}$$

Chemotactic flux - which we consider caused solely by the production of attractant - follows by integrating $D_2 v_{rr} \sim \alpha u$ to get $v_r \sim \alpha D_2^{-1} \int u\, dr \sim \alpha D_2^{-1} M^{1D}$. The chemotactic flux becomes

$$J_2 \sim \chi u v_r \sim \alpha \chi u M^{1D} D_2^{-1} \tag{3.47}$$

If the system collapses onto a plane, the thickness of the sheet $l \to 0$. This makes the diffusive flux J_1 explodes (because of division by zero) while the chemotactic flux J_2 is unchanged. Hence the plane with small thickness is unable to reach infinite density, because diffusion dominates and eventually stops the collapse.

For higher dimension space, the chemotactic flux of symmetric spherical collapse is singular. By balancing $D_2 \Delta v \sim \alpha u$, we get $(r^2 v_r)_r \sim \alpha r^2 u D_2^{-1}$ which

implies a concentration gradient $v_r \sim \alpha M^{3D}(l^2 D_2)$. The net inward flux of cells in higher space dimension becomes

$$J_1 \sim \frac{-D_1 u}{l} + \frac{\alpha \chi u M^{3D} D_2^{-1}}{l^2} \tag{3.48}$$

In this equation we can see the domination of inward flux (second term) as $l \to 0$ which then causes collapse.

For the borderline case in two dimensions, by $(rv_r)_r \sim \alpha r u D_2^{-1}$, the inward flux is

$$J_1 \sim \frac{-D_2 u + \alpha \chi u M^{2D} D_2^{-1}}{l} \tag{3.49}$$

The chemotactic and diffusive fluxes scale the same way with l. If $M^{2D} > D_1 D_2/(\alpha\chi)$, there is a net inward flux which suggests that a system with mass above this critical value collapse.

See articles by Miguel A. Herrero et. al. (9), Herrero and Velázquez (10) (11), Jäger and Luckhaus (19), and Nagai (27) (26) for further studies of blow up and its dependence on space dimensions.

3.4 Modified Keller-Segel Model

Since the results by Jäger and Luckhaus, blow up solutions have been quite well understood and there are scores of literature on blow up solutions. The historical development of the Keller-Segel model with blow up is summarized by Dirk Horstmann (18) in two reviews.

However, the scene of blow up (particularly in slime mold amoebae *D. discoideum*) is still obscure and mathematicians have various interpretations of blow up into its biological aspects. Herrero and Velázquez consider blow up as a simplified model for the formation of sporae while Hillen and Painter interpret the aggregation and formation of fruiting body for sporae as a mechanism of blow up prevention.

As it has been elucidated in Chapter 2 previously, chemotaxis also plays eminent role in inflammation. Chavez-Ross et. al. (5) and references therein explain about entanglement of chemotactic behaviour of glial (nonneural) cells and Alzheimer's disease (AD). The cells, microglia and astrocytes, activate when there

exist inflammation, which causes cells to proliferate and migrate chemotactically to sites of injury where they secrete a host of chemicals, including cytokinesis. Microglia, which is 10 - 15 μm in size, distributed sparsely in the brains of healthy individuals (e.g., 0.3 cells per $10^4 \mu m^2$ in temporal neocortex), but found at much higher densities in AD (between 100 and 350 reactive microglia cells in a section $10^4 \mu m^2$ in area and 30μm thick in a hippocampus of an Alzheimer's patient). This high density is deemed to result from aggregation of chemotaxis.

We may deduce that some cells possess a mechanism to obstruct population overcrowding while some cells unfortunately don't, as we can see from the case of Alzheimer's disease above. Therefore it is interesting to study mechanisms that could prevent collapse of the cell density. Hillen[1] suggests various types:

1. Saturation effects,
2. Volume filling effects,
3. Quorum sensing effects,
4. Finite Sampling radius.

We are interested in the volume-filling effects which are a mechanism of finite size of individual cells. In this approach, assumption is put on the probability of making a jump that depends upon the availability of space into which cells can move. It has been delineated by Painter and Hillen, in volume-filling mechanism cells are chemotactically migrating towards an increasing attractant gradient. Consider figure (3.1).

Cell A is in a low density region and can move freely to any direction though the chemosensitive bias is to the right. Cell B, on the other hand, is in a semi-packed environment is inhibited moving to the right due to the lack of space, although it experiences a bias to that direction. Cell C is completely seized on all directions, and unable to move.

In this mechanism, chemotaxis equations are derived from reinforced random walk motions proposed by Othmer and Stevens (29) which are then used to get a set of continuum models to describe cell movement. Othmer and Stevens

[1] http://www.math.ualberta.ca/~thillen/chemotaxis.html

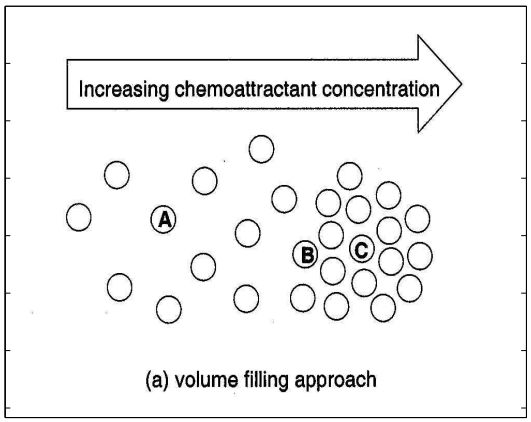

Figure 3.1: Volume-filling mechanism, taking from Hillen & Painter's article (16)

introduce master equation for a continuous-time, discrete-space random walk on a one-dimensional domain of equidistant lattice (though the derivatives extend to higher dimensions without change and the general result in each case is usually simplified). This description was labelled a *space-jump process*. Suppose $u_i(t)$ is defined as the conditional probability of a walker (or cell) to be at $i \in \mathbb{Z}$ at time t, conditioned on beginning at $i = 0$ at $t = 0$ and it evolves according to the continuous-time discrete space master equation and by restricting attention to one-step jump,

$$\frac{\partial u_i}{\partial t} = \mathcal{T}^+_{i-1}(W)u_{i-1} + \mathcal{T}^-_{i+1}(W)u_{i+1} - (\mathcal{T}^+_i(W) + \mathcal{T}^-_i(W))u_i \tag{3.50}$$

where $\mathcal{T}^\pm_i(\cdot)$ are the *transitional-probabilities* per unit time of a one-step jump to $i \pm 1$, and $(\mathcal{T}^+_i(W) + \mathcal{T}^-_i(W))^{-1}$ is the main waiting time at the ith site. These are assumed nonnegative and suitably smooth functions. The vector W is given by

$$W = (..., w_{-i-1/2}, w_{-i}, w_{-i+1/2}, ..., w_0, w_{1/2}, ...) \tag{3.51}$$

where w is the control species defined on the lattice of half the step size.

The model of equation (3.50) simply describes the changing particle/cell numbers as individuals enter or leave a site.

The decision of when and where to jump is relied upon additional factors, such as external concentration of a chemical substances. Thus we have a spatial-bias

in the random walk which we assume to be caused by v, a vector representing the chemical concentration and defined in the similar way as W above. Then, $\mathcal{T}_i^{\pm} = \mathcal{T}_i^{\pm}(v)$.

The cell movement can be modelled by dividing the one-dimensional lattice into a finite segment $(-N, N)$. We extend u and v as even functions about $-N$ and N. The net flux across the boundary under suitable conditions on $\mathcal{T}$ can be ensured to be zero in the continuum limit of the one-dimensional problem, and this will yield a conserved mass.

Painter and Sherratt in (32) describe various types of models of biased movement of a cell on a lattice, where the jump probabilities depend on a variety of environmental factors (e.g. other cell populations or chemical concentrations). Those sensing strategies are:

1. *Strictly local model* : information only at the present position is considered. By choosing $\mathcal{T}_i^{+} = \mathcal{T}_i^{+} = f(v_i)$ where v_i represents the information at i (or, in our case, the chemical attractant), the master equation becomes

$$\frac{\partial u_i}{\partial t} = f(v_{i+1})u_{i+1} - 2f(v_i)u_i + f(v_{i-1})u_{i-1} \tag{3.52}$$

and under appropriate scalling, the continuum model of PDE is derived

$$\frac{\partial u}{\partial t} = D\frac{\partial^2}{\partial x^2}(f(v)u) \tag{3.53}$$

2. *Neighbour based model* : considers information at the target jump site. Here the $\mathcal{T}_i^{\pm} = g(v_{i\pm1})$ and results in for the master equation

$$\frac{\partial u_i}{\partial t} = g(v_i)(u_{i+1} + u_{i-1}) - u_i(g(v_{i+1}) + g(v_{i-1})) \tag{3.54}$$

and in the PDE limit

$$\frac{\partial u}{\partial t} = \frac{\partial}{\partial x}\left[g(v)\frac{\partial u}{\partial x} - u\frac{\partial g(v)}{\partial x}\right] \tag{3.55}$$

For decreasing g, this models processes such as "space-limitation", where a cell is only able to move into a neighbouring site if there is sufficient space available.

3. *Local average model* : considers the average of the information between the particles present and target site. By assuming $\Upsilon_i^{\pm} = h((v_{i\pm1} + v_i)/2)$, the master equation becomes

$$\frac{\partial u_i}{\partial t} = h\left(\frac{v_{i+1} + v_i}{2}\right)(u_{i+1} - u_i) - h\left(\frac{v_i + v_{i-1}}{2}\right)(u_i - u_{i-1}) \tag{3.56}$$

and the PDE is derived as

$$\frac{\partial u}{\partial t} = \frac{\partial}{\partial x}\left(h(v)\frac{\partial u}{\partial x}\right) \tag{3.57}$$

4. *Gradient based model* : this model assumes transitional probabilities of the form

$$\Upsilon_i^{\pm} = \omega + \varphi(\tau(v_{i\pm1}) - \tau(v_i)) \tag{3.58}$$

where τ represents the mechanism of signal detection. The resulting PDE is

$$\frac{\partial u}{\partial t} = \frac{\partial}{\partial x}\left[D\frac{\partial u}{\partial x} + u\frac{d\tau}{dv}\frac{dx}{dx}\right] \tag{3.59}$$

5. *Combined model* : a combination of the previous models may be necessary to most accurately reflect cell movement. The master equation becomes

$$\Upsilon_i^{\pm} = f(v_i)g(v_{i\pm1})(\omega + \varphi(\tau(v_i) - \tau(v_{i\pm1}))) \tag{3.60}$$

and the PDE corresponding to this combined movement rule is

$$\frac{\partial u}{\partial t} = \frac{\partial}{\partial x}\left[g(v)\frac{\partial}{\partial x}(f(v)u) - f(v)u\frac{\partial g(v)}{\partial x} + ug(v)f(v)\frac{d\tau}{dv}\frac{dv}{dx}\right] \tag{3.61}$$

For the interaction of two cell populations, or interaction between cells and a chemical substance, the corresponding equations would be as follow

$$\begin{aligned}
\frac{\partial u}{\partial t} &= \frac{\partial}{\partial x}\left(f(v)\frac{\partial u}{\partial x} + u\frac{\partial f(v)}{\partial v}\frac{\partial v}{\partial x}\right) \quad -- \textit{Strictly local model},\\
\frac{\partial u}{\partial t} &= \frac{\partial}{\partial x}\left(g(v)\frac{\partial u}{\partial x} - u\frac{\partial g(v)}{\partial v}\frac{\partial v}{\partial x}\right) \quad -- \textit{Neighbour based model},\\
\frac{\partial u}{\partial t} &= \frac{\partial}{\partial x}\left(h(v)\frac{\partial u}{\partial x}\right) \quad -- \textit{Local average model},\\
\frac{\partial u}{\partial x} &= \frac{\partial}{\partial x}\left(D\frac{\partial u}{\partial x} + u\chi(v)\frac{\partial v}{\partial x}\right) \quad -- \textit{Gradient based model}.
\end{aligned} \tag{3.62}$$

where here u denotes the density of the cells (or one of the densities in the case of two interacting species), and v denotes the concentration of the chemical attractant or the other cell density.

Meanwhile, thinking about how the total cell density can affect the movement properties of the cells, there are (so far) three models that are led to dispersal of the population:

1. "Population pressure" – A high cell density results in increased probability of a cell being "pushed" from a site, for example due to the pressure exerted by neighbouring cells. This might be achieved using the strictly local formulation and $f(v)$ increasing.

2. "Limited space" – No more cells can enter a site above a total cell density. This may be achieved either the neighbour or local average-based model, and choosing $g(v)$ or $h(v)$ such that there exists some T for which $g(T) = 0$ when $v = T$.

3. "Gradient detection" – Cells may detect and respond to a local gradient in the cell density, achieved by the gradient-based model. This model has been employed extensively in chemotaxis. To ensure that cells move down gradients in the total density, we require $\chi(v) > 0$.

For the chemotaxis with volume-filling mechanism, we use the gradient detection model, where we assume that before making decision of moving, cells examine the environment by detecting the difference between v at the current point (v_i) and the the nearest neighbour ($v_{i\pm1}$) in the direction of movement. For simplicity, only linear dependence on nearest-neighbour differences can be treated, as in equation (3.58). For the transitional probabilities of that form, $\omega \geq 0$ and φ are constants, ω is not small compared to φ and the variations $\tau(v_{i\pm1}) - \tau(v_i)$ are not too large.

We consider $q(u)$ as the probability of the cell finding space at its neighbouring location. By assuming that the probability of jumping into a neighbouring site is dependent upon the amount of space available at that site, the transitional probabilites for this model become (16)

$$\mathcal{T}_i^{\pm} = q(u_{i\pm1})(\omega + \varphi(\tau(v_{i\pm1}) - \tau(v_i))) \tag{3.63}$$

Substituting equation (3.63) into the master equation (3.50), gives

$$\begin{aligned}\frac{\partial u_i}{\partial t} &= q(u_i)\left[\omega+\varphi(\tau(v_{i+1})-\tau(v_i))\right]u_{i-1}+q(u_i)\left[\omega+\varphi(\tau(v_i)-\tau(v_{i+1}))\right]u_{i+1}\\ &\quad -\left[q(u_{i+1})(\omega+\varphi(\tau(v_{i+1})-\tau(v_i)))+q(u_{i-1})(\omega+\varphi(\tau(v_{i-1})-\tau(v_i)))\right]u_i\\ &= \omega\left[q(u_i)u_{i-1}+q(u_i)u_{i+1}-(q(u_{i+1})+q(u_{i-1}))u_i\right]\\ &\quad +\varphi(q(u_i)(\tau(v_i)-\tau(v_{i-1}))u_{i-1}+q(u_i)(\tau(v_i)-\tau(v_{i+1}))u_{i+1}\\ &\quad -q(u_{i+1})(\tau(v_{i+1})-\tau(v_i))u_i-q(u_{i-1})(\tau(v_{i-1})-\tau(v_i))u_i) \end{aligned} \tag{3.64}$$

We set $x=ih$, reinterpret x as a continuous variable and extend the definition of u_i accordingly. As the spatial scale, h, is changed, the transitional probabilities to jump to a neighbouring location must depend on that scale. For some scaling constant k, it is assumed that $\mathcal{T}_h^{\pm}=\frac{k}{h^2}\mathcal{T}^{\pm}$. And as the right hand side in powers of h is expanded, we obtain for the density $u(x,t)$ in continuum PDE

$$\frac{\partial u}{\partial t}=k\omega\left(q(u)\frac{\partial^2 u}{\partial x^2}-u\frac{\partial^2 q(u)}{\partial x^2}\right)-2k\varphi\frac{\partial}{\partial x}\left(q(u)u\frac{\partial\tau(v)}{\partial x}\right)+\mathcal{O}(h^2) \tag{3.65}$$

in the limit of $h\to 0$, divergence form reads

$$\frac{\partial u}{\partial t}=\frac{\partial}{\partial x}\left(D_1(q(u)-q'(u)u)\frac{\partial u}{\partial x}-q(u)u\chi(v)\frac{\partial v}{\partial x}\right) \tag{3.66}$$

where

$$D_1=k\omega \qquad \text{and} \qquad \chi(v)=2k\varphi\frac{d\tau(v)}{dv} \tag{3.67}$$

The diffusion term of this form looks similar to that of *Porous Media Equation* (PME). The application of PME to biological populations has been studied by Gurtin and MacCamy (8). Adopting Gurtin and MacCamy assumption to use increasing function in the diffusivity when populations behave so as to avoid crowding, we relate to the model in equation (3.66) that $q(u)-q'(u)u$ is supposed to be an increasing function.

For this purpose, *Allee Effect* in model of population dynamics can be one logical choice for $q(u)$, with its simplest form (6)

$$q(u)=2-(u-1)^2 \tag{3.68}$$

Allee effect represents a population that has a maximal intrinsic growth rate at intermediate density, as in figure (3.2).

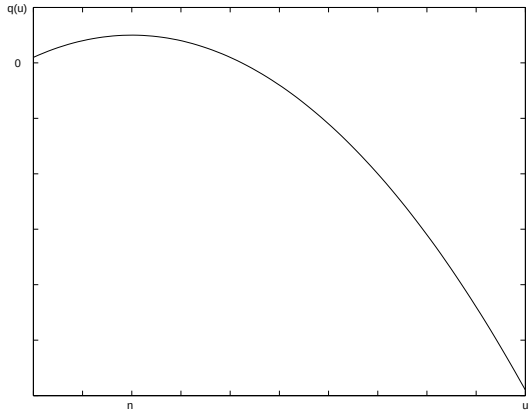

Figure 3.2: Allee effect

Clearly by using equation (3.68), then we have $q(u) - q'(u)u = u^2 + 1$ which is of parabolic in increasing form.

Another choice for $q(u)$ suggested by Painter and Hillen in (16) is

$$q(u) = 1 - \frac{u}{U_{max}}, \tag{3.69}$$

which states that the probability of a jump into a site decreases linearly with the cell density at that site.

The density equation interpreted as a limiting equation for moderately interacting cells may depend strongly on the dynamics of v, the chemical substance. In particular, the growth of v determines whether or not blowup occurs. One realistic type of dynamics for v is *saturating growth*. We borrow a model from *Michaelis-Menten Kinetics* which is based on the fact that bacterial growth rates may depend on nutrient availability. The mechanism is also known as *Saturating Nutrient Consumption Rate*, explained as below. For low level of the nutrient concentration c, bacterial growth rate given by equation (3.70) below is roughly proportional to c. At high level of c, this rate approaches a constant value K_{max}. The saturating kinetics that are exhibited by numerous biological phenomena formulated as

$$K(C) = \frac{K_{max}C}{K_n + C} \tag{3.70}$$

and illustrated in figure (3.3)

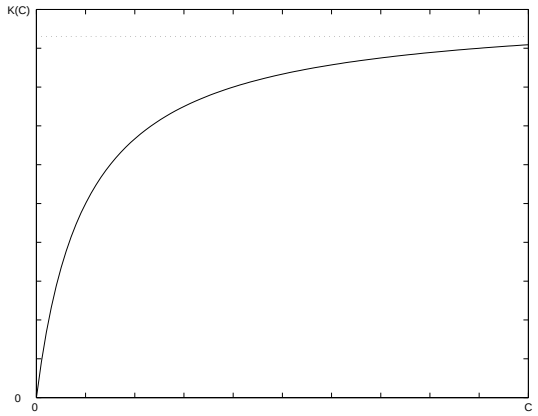

Figure 3.3: Michaelis-Menten kinetics

We incorporate the "volume-filling" using Allee effect and "Michaelis-Menten kinetics" in our modified Keller-Segel equations which become

$$u_t = \nabla \cdot (D_1(u^2+1)\nabla u) - \nabla \cdot (\chi u(2-(u-1)^2)\nabla v)\,, \tag{3.71}$$

$$v_t = D_2 \Delta v + \frac{\epsilon u}{1+u} - \beta v\,. \tag{3.72}$$

3.4.1 Steady State Analysis for the Modified Keller-Segel Model

We study the steady state of the modified equations in one dimension on the interval $[0, L]$ with zero flux boundary conditions, as given in (16). The cell density for our new modified model evolves according to the equation (3.71). Setting $u_t = 0$ leads to

$$\left(D_1(u^2+1)u_x - \chi u(2-(u-1)^2)v_x\right)_x = 0 \tag{3.73}$$

Integrating once then results in

$$\mathbf{J} = \text{constant} \tag{3.74}$$

where $\mathbf{J}$ is cell flux, the expression in parenthese in equation (3.73). If the equation (3.73) is confined to the domain $[0, L]$ with the no-flux boundary conditions, then $\mathbf{J}= 0$ at $x = 0$ implies that $\mathbf{J} \equiv 0$ for all x. Thus

$$D_1(u^2+1)u_x - \chi u(2-(u-1)^2)v_x = 0 \tag{3.75}$$

or

$$D_1(u^2+1)u_x = \chi u(2-(u-1)^2)v_x \tag{3.76}$$

We obtain

$$u_x = \mu(x)\frac{u(2-(u-1)^2)}{u^2+1} \tag{3.77}$$

where

$$\mu(x) = \frac{\chi}{D_1}v_x \tag{3.78}$$

If we use the general $q(u)$ in equation (3.77) and might arrange it into ordinary form

$$\frac{du}{dx} = \mu(x)\frac{q(u)u}{q(u)-q'(u)u} \tag{3.79}$$

this equation can be solved using method separation of variables by equating all terms with dependent variable u to the left and integrate

$$\int \frac{q(u)-q'(u)u}{u\,q(u)}\,du \sim c \tag{3.80}$$

and equating terms with x to the right hand side, yields

$$M(x) \sim \int \mu(x)dx = \frac{\chi}{D_1}v(x) \tag{3.81}$$

Solving (3.80), we have

$$\frac{u}{q(u)} = c\,e^{M(x)} \tag{3.82}$$

where $M(x)$ as in equation (3.81), and c can be specified using conservation of mass

$$\int_0^L u(x)\,dx = \bar{U}_0 = \int_0^L u_0(x)\,dx \tag{3.83}$$

If we represent the left hand side of equation (3.82) by

$$\Psi(u) := \frac{u}{q(u)} \tag{3.84}$$

and we consider $q(u)$ to be decreasing function (including our chosen model), then

$$\Psi'(u) = \frac{q(u)-u\,q'(u)}{(q(u))^2} > 0 \tag{3.85}$$

Hence Ψ is strictly increasing and invertible, and Ψ^{-1} is also strictly increasing. Therefore the solution of (3.79) is given by

$$u = \Psi^{-1}\left(c\, e^{M(x)}\right) \tag{3.86}$$

The steady state of chemical attractant equation is solved by setting $v_t = 0$, hence

$$D_2 v_{xx} - \beta v = -\frac{\epsilon u}{1+u} \tag{3.87}$$

which is an elliptic boundary value problem. We can solve the equation that is similar to the inhomogeneous 2nd-order differential equations by

$$v(x) = \mathcal{A}e^{m_1 x} + \mathcal{B}e^{m_2 x} - \frac{\epsilon}{D_2}\frac{u}{1+u} \tag{3.88}$$

with u as in equation (3.86), we get m_1 and m_2 from integrating factor of the equation.

3.5 Finite Element Method

In this section, we develop the Finite Element Method using approximations consist of continuous piecewise linear functions in space and discontinuous polynomials of degree 0 in time, which is called cG(1)dG(0) method or the *Backward Euler* method for the Keller-Segel models occupy homogeneous Neumann boundary conditions.

Let $I = [0, T_{max}]$ be the given time interval and we discretize it on a subdivision $0 = t_0 < t_1 < ... < t_N = T_{max}$ into sub-intervals $I_n = (t_{n-1}, t_n]$ of length $k_n = t_n - t_{n-1}$.

We give the Keller-Segel equations (3.10) and (3.11) the following variational formulation by multiplying the equations with the so-called *test functions* $w = w(x,t) \in H^1$ such that

$$(u_t, w) + (D_1 \nabla u, \nabla w) = (\chi u; \nabla v, \nabla w) \quad \forall\, w \in H^1 \tag{3.89}$$

$$(v_t, w) + (D_2 \nabla v, \nabla w) + (\beta v, w) = (\alpha u, w) \quad \forall\, w \in H^1 \tag{3.90}$$

where

$$(u, w) = \int_{I_n}\int_{\Omega} u\, w\, d\Omega\, dt$$

$$(\nabla u, \nabla w) = \int_{I_n} \int_{\Omega} \nabla u \cdot \nabla w \, d\Omega \, dt$$

$$(\chi u; \nabla v, \nabla w) = \int_{I_n} \int_{\Omega} \chi u \nabla v \cdot \nabla w \, d\Omega \, dt$$

and

$$H^1 = \{w : \int_{\Omega} (|\nabla w|^2 + w^2) \, dx < \infty\} \tag{3.91}$$

and the boundary conditions $\partial_n u = 0$ and $\partial_n v = 0$ on $\partial\Omega$ were used to eliminate the boundary integral over $\partial\Omega$ due to the Green's formula

$$\int_{\Omega} \Delta u \, w \, dx = \int_{\partial\Omega} \partial_n u \, w \, ds - \int_{\Omega} \nabla u \cdot \nabla w \, dx \tag{3.92}$$

We take Ω to be a bounded domain in $\mathbb{R}^2$ and assume the boundary $\partial\Omega$ to be smooth. Let us now construct a finite-dimensional subspace $W_h \subset H^1$. The domain is discretized by a mesh of triangular elements in the $x-$ and $y-$directions by subdividing Ω into a set $\mathcal{T}_h = K_1, ..., K_m$ of non-overlapping triangles K_i,

$$\Omega = \bigcup_{K \in \mathcal{T}_h} K = K_1 \cup K_2 ... \cup K_m$$

such that there is no vertex of one triangles lies on the edge of another triangle, and the mesh parameter

$$h = \max_{K \in \mathcal{T}_h} \text{diam}(K)$$

$$\text{diam}(K) = \text{diameter of } K = \text{longest side of} K$$

We now define W_h as follows

$$W_h = \{w : w \text{ is continuous on } \Omega, \ w|_K \text{ is linear for } K \in \mathcal{T}_h\}$$

The space W_h consists of all continuous functions that are linear on each triangle K.

For the Backward Euler method, we replace the time derivative u_t by the difference quotient $(u_n - u_{n-1})/k_n$, see (20). The discretized finite element method for the original Keller-Segel model reads: Find $U_n \in W_h$ and $V_n \in W_h$, $n = 0, 1, ..., N$ such that

$$\int_{\Omega} U_n w \, dx + k_n \int_{\Omega} D_1 \nabla U_n \cdot \nabla w \, dx = \int_{\Omega} U_{n-1} w \, dx + k_n \int_{\Omega} \chi U_n \nabla V_n \cdot \nabla w \, dx \tag{3.93}$$

$$\int_\Omega V_n w\,dx + k_n \int_\Omega D_2 \nabla V_n \cdot \nabla w\,dx + k_n \int_\Omega \beta V_n w\,dx = \int_\Omega V_{n-1} w\,dx + k_n \int_\Omega \alpha U_n w\,dx \tag{3.94}$$

where U_n denotes the value at $t = t_n$ and U_{n-1} denotes the value at $t = t_{n-1}$, and $g(U_n) = \epsilon U_n/(U_n + 1)$. And the finite element method for the modified Keller-Segel model of equations (3.71) and (3.72) follows

$$\int_\Omega U_n w\,dx + k_n \int_\Omega D_1(q(U_n) - q'(U_n)U_n)\nabla U_n \cdot \nabla w\,dx = \int_\Omega U_{n-1} w\,dx + k_n \int_\Omega \chi U_n \nabla V_n \cdot \nabla w\,dx \tag{3.95}$$

$$\int_\Omega V_n w\,dx + k_n \int_\Omega D_2 \nabla V_n \cdot \nabla w\,dx + k_n \int_\Omega \beta V_n w\,dx = \int_\Omega V_{n-1} w\,dx + k_n \int_\Omega \left(\frac{\epsilon U_n}{U_n + 1} w\right) dx \tag{3.96}$$

Chapter 4

Numerical Applications

4.1 Meshing

We take for Ω the square domain of $L \times L$.

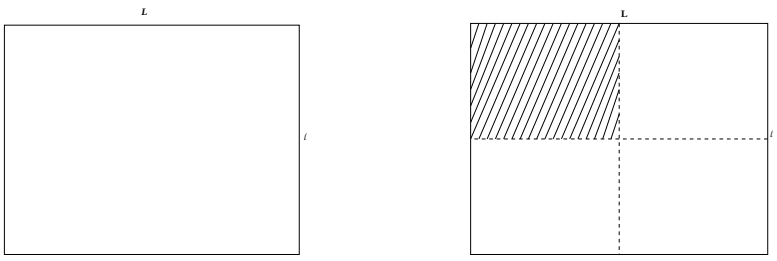

Figure 4.1: Domain and reduction by symmetry

By reason of symmetry we consider only a quarter of the domain Ω, namely $(L/2, L/2)$, then the boundary conditions of symmetry $\partial\Omega_s$

$$\begin{aligned} \frac{\partial u}{\partial n} &= 0 \quad \text{on} \quad \partial\Omega_s\,, \\ \frac{\partial v}{\partial n} &= 0 \quad \text{on} \quad \partial\Omega_s\,. \end{aligned} \tag{4.1}$$

The simulations were performed by the commercial finite element code FEMLAB on a PC with processor 1.7 GHz and 256 MB of RAM. The mesh triangulation is generated using Delaunay/Voronoi triangulation. In all numerical simulations, two meshes have been used in order to see if the spatial discretization might affect the transient, as they are shown in figures (4.2) for domain Ω

= square = 1×1. The two meshes are different in the growth rate. For the first mesh we choose its mesh growth rate to be 1.2 and for the second mesh is 1.07. Each mesh refinement is jiggled two times. We use as small as possible time step, that is $k = 0.0001$ from $k = h^2$ where h is the longest side of the smallest element, for all simulations.

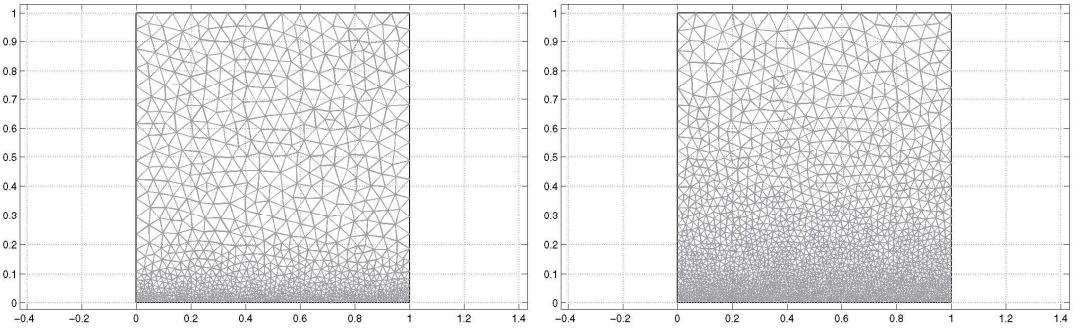

Figure 4.2: Square symmetrical meshes

The first mesh, as shown in the left part of figure (4.2), has 1112 nodes and 2065 elements. And the second mesh on the right side consists of 2230 nodes and 4283 elements.

It has been acknowledged in all literature about the Keller-Segel model, that the solutions of the nonlinear strongly-coupled equations might result in sharp gradients (or "spike") that can pose stability problems in numerical methods. Or, we consider as "blow up" in the previous section. We will see the sharp gradients near the area of the center of aggregation in our simulations later. Here we assume that we already have *a priori* knowledge of where the aggregations form, by refining the mesh around the area.

For all simulations in this section, we choose an arbitrarily smooth function for the initial value of the cells, $u_0 = 0.5 - 0.1y$, and about the homogeneous steady state for the chemical concentration v_0. Other physical parameters are also chosen arbitrarily following the conditions given in inequality (3.41), $D_1 = 0.0001, D_2 = 0.01, \alpha = 1$, and $\beta = 0.1$.

4.2 Simulations of The Keller-Segel Model

In this part, we take $L = l = 1$ length unit. We show the results for equations (3.10) and (3.11) that yield sharp gradients after some finite time.

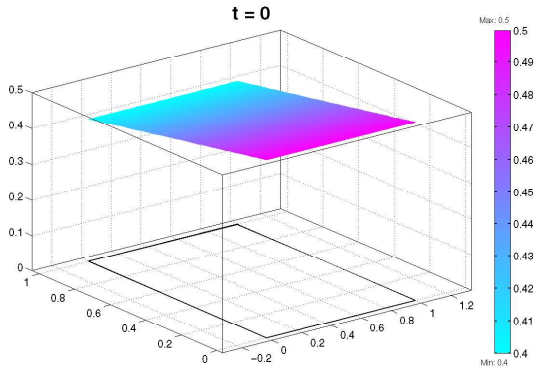

Figure 4.3: At initial condition t = 0

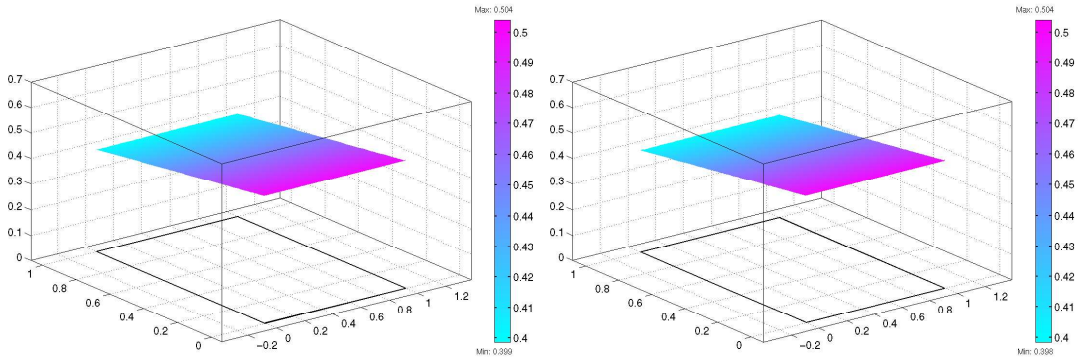

Figure 4.4: Bacteria concentration after numerical time t = 50

At initial state $t = 0$, due to the initial condition of u_0, the solutions show linear increase from the boundary of domain to the center by 0.1 difference. In the figure (4.4), at $t = 50$ the solutions on the boundary of main domain tend to decrease while the solutions near the center increase.

At numerical time $t = 100$, we see the solutions near the center start to oscillate. This is when the numerical instability starts to grow. And peaks or sharp gradients are distinct when the solutions reach time $t = 174$ for the first

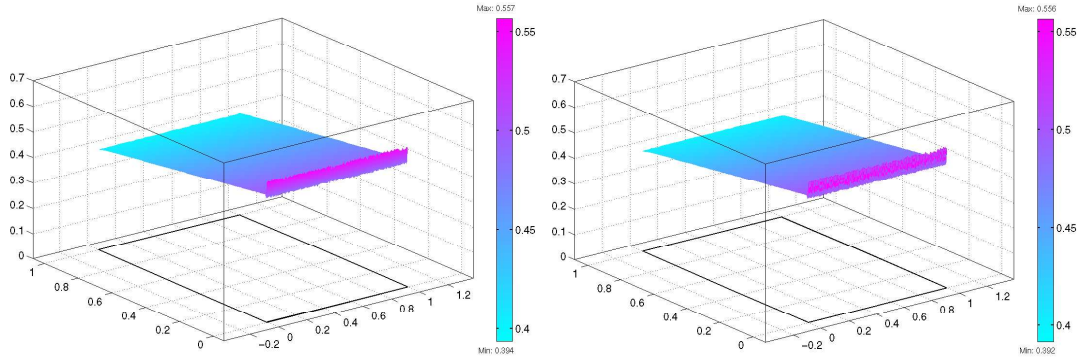

Figure 4.5: Bacteria concentration after numerical time t = 100

mesh (on the left side) or at $t = 173$ for the second mesh (on the right side) of figure (4.6). Here we see the solutions oscillate and reach negative values. The negative might be due to the difficulty of the numerical software to meet integration tolerances and it requires smaller step size to cope with.

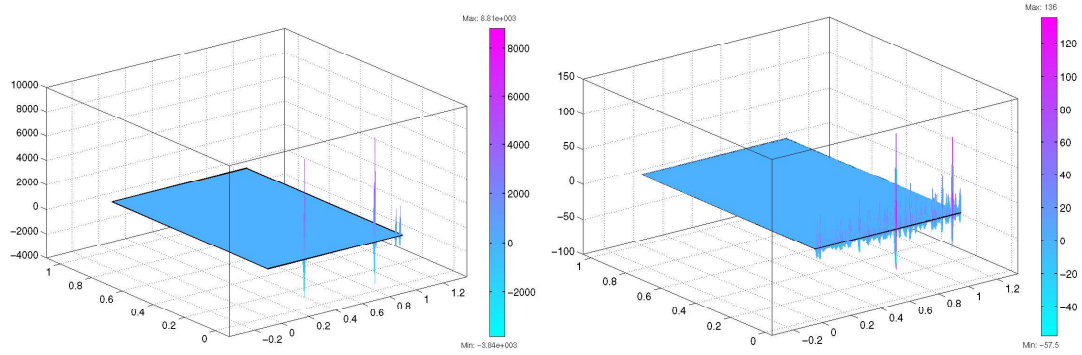

Figure 4.6: Very high sharp gradients after numerical time t = 174

Cross section views of the solutions at $t = 50, t = 100$ are as seen in figure (4.7) and (4.8). The solutions continue to evolve in a manner leading to the disappearance of number of peaks. At $t = 174$ the peaks collapse into one or two peaks which continue growing. The cross section for the chemical attractant at the same numerical time is shown in figure (4.10)

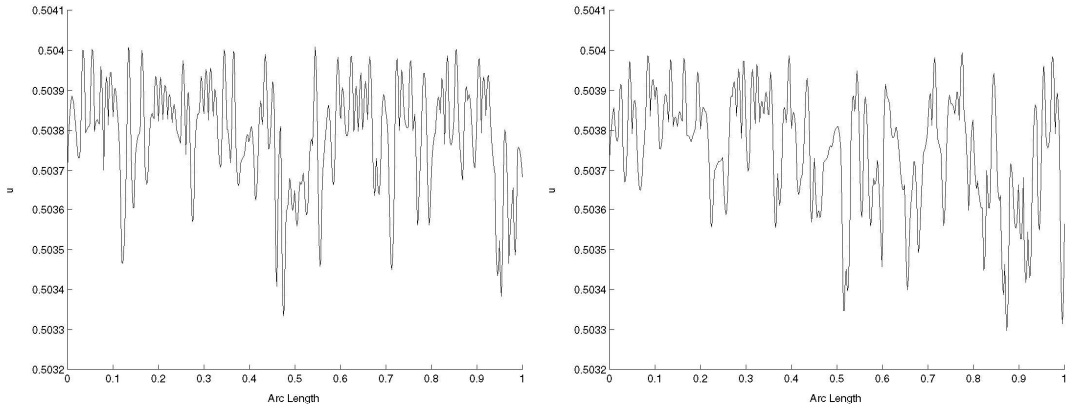

Figure 4.7: Cross section view of the cell concentration equation at t = 50

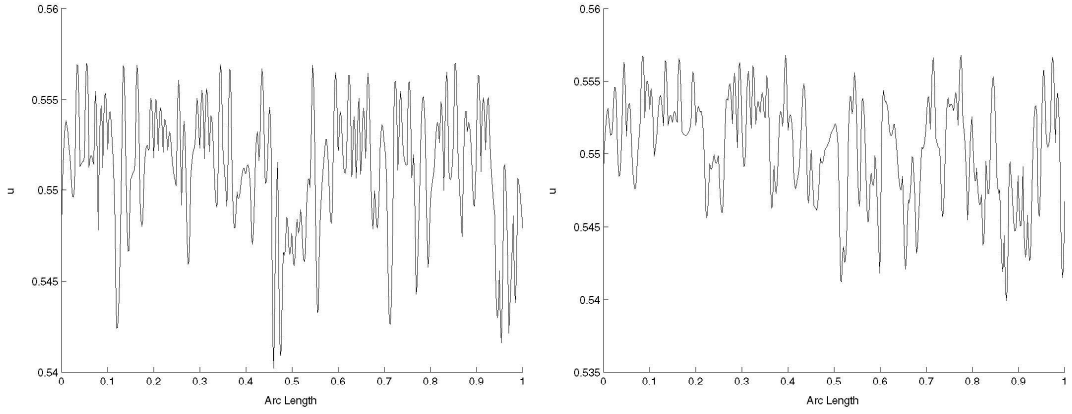

Figure 4.8: Cross section view of the cell concentration equation at t = 100

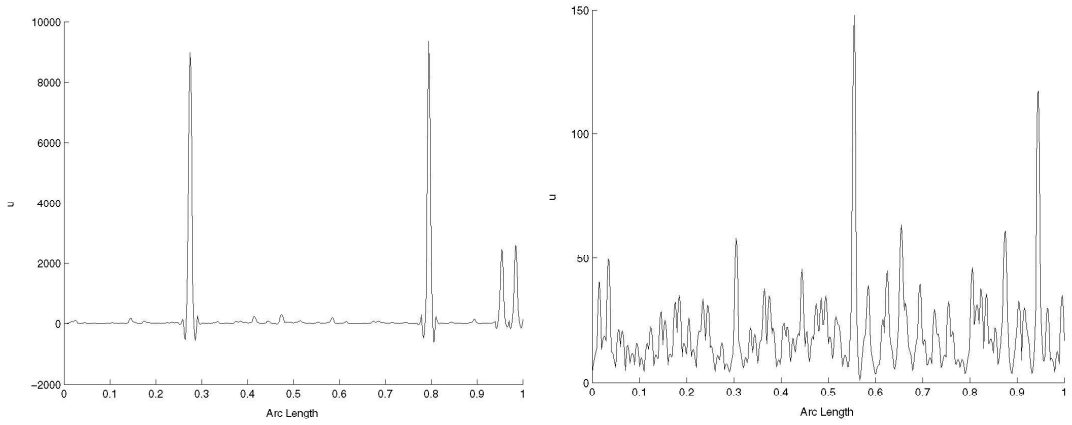

Figure 4.9: Cross section view of the sharp gradients of cell concentration equation at t = 174

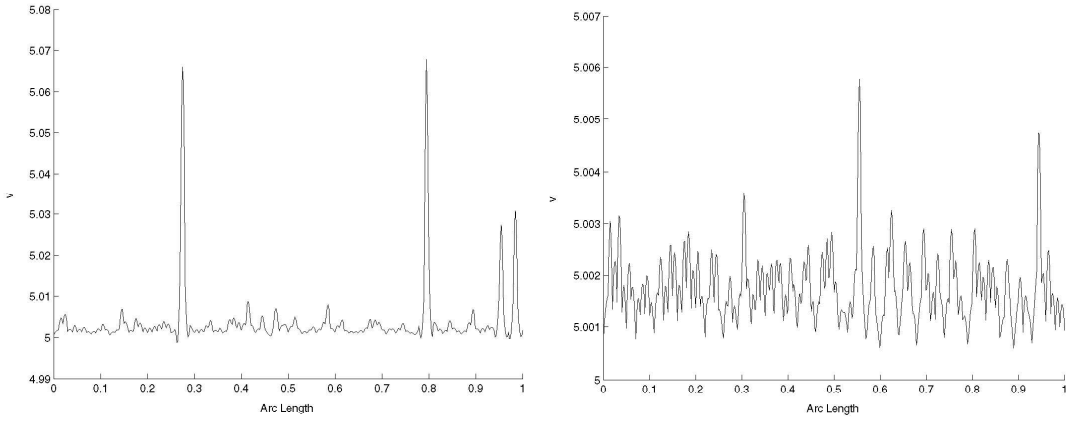

Figure 4.10: Cross section view of the chemical attractant at numerical time with peaks

4.3 Simulations of the Modified Keller-Segel Model

With similar domain as in previous section, here we show the results of the modified Keller-Segel equations (3.71) and (3.72) using Allee effect and Michaelis-Menten kinetics. Arbitrarily, with the same parameters for diffusive coefficients, we pick $\epsilon = 0.1$ for the Michaelis-Menten kinetics equation of the chemical attractant.

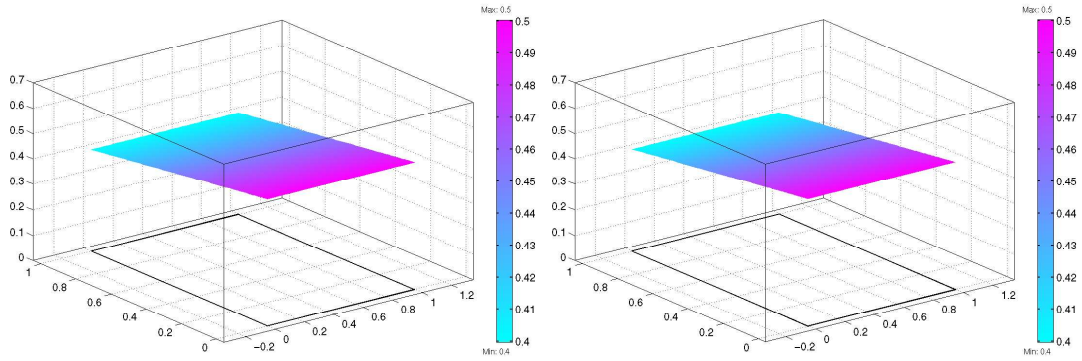

Figure 4.11: Bacteria concentration simulation with modified Keller-Segel equations after numerical time t = 100

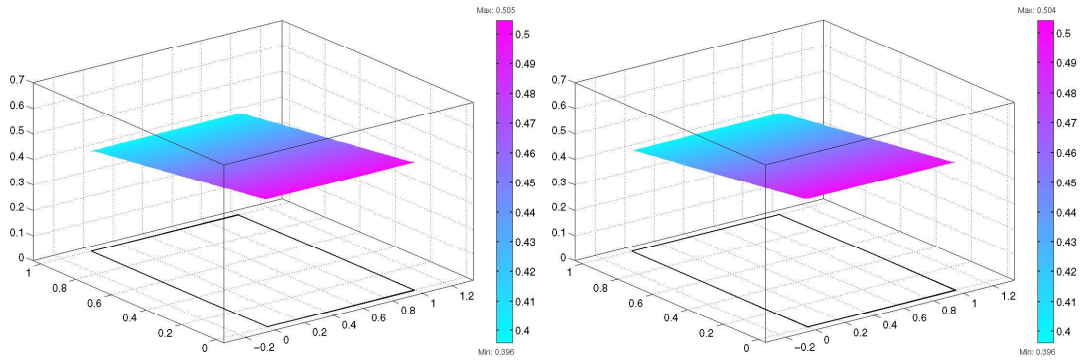

Figure 4.12: Bacteria concentration simulation with modified Keller-Segel model after numerical time t = 500

At time $t = 100$, the solutions slightly move from the initial condition. And after $t = 500$, we can see slow increment of the solutions, which indicates the starting of the inequality in equation (3.41). The solutions at numerical time

$t = 1000$ are shown in figure (4.13). Here, at the center of aggregation, the cell concentration moves up in such a way of not to cause overcrowding or peaks of solutions.

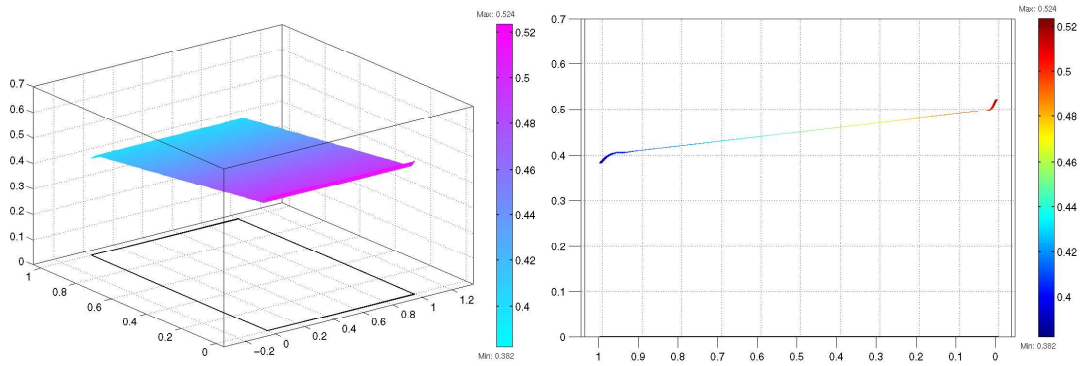

Figure 4.13: Bacteria concentration after numerical time t = 1000 (left figure), and the cross section view (right figure)

Chapter 5

Review of Chemotaxis Models

The Keller-Segel model that underlies chemotaxis has been studied and analyzed from both microscopic (stochastical) approach and macroscopic approach. The basis equations, or classical Keller-Segel equations,

$$\begin{aligned} u_t &= \nabla \cdot (D_1(u,v)\nabla u) - \nabla \cdot (\chi(u,v)u\nabla v) + f(u,v) \\ v_t &= \nabla \cdot (D_2(u,v)\nabla v) + \alpha(u,v)u - \beta(u,v)v \end{aligned} \tag{5.1}$$

is a system that has a rich dynamics and possible behaviours of the solutions include convergence to time independent solutions and the formation of finite time blow up. The blow up is widely reckoned to depend on space dimensions, in radially symmetric and nonsymmetric solutions.

5.1 Reviews from The Macroscopic Approach

Schaaf in (5) in 1985 discussed the following forms of chemotactic sensitivity as function of chemical: (1) $\chi(v) = \chi =$ constant, (2) $\chi(v) = 1/v$ known as *log form*, and (3) a *receptor-kinetics form* $\chi = 1/(k+v)^2$, where $k > 0$.

Post in (33) studied chemotaxis using Lyapunov function by assuming the chemotactic sensitivity in the form of $\tilde{\chi}(v) = \chi S'(v)$ and $\tilde{\delta}(v) = \delta S'(v)$ where $S'(v)$ denotes the first derivative of S (sensitivity funtion) with respect to v.

Rivero, also cited in (5), in 1989 discussed the dependence of diffusion coefficient on chemical attractant $D(v)$.

Some models consider v_t to be equal to zero by borrowing the results of biological experiments in semisolid agar, where the diffusion of bacteria is founded

slower than attractant diffusion, as modelled by Brenner and Betterton in (2), Brenner et. al. in (3), Marrocco in (23), Chalub et. al. in (4), Herrero and Velázquez in (10) (9), Herrero et. al. in (9), and Nagai and Senba in (27).

This macroscopic approach using continuum reaction-diffusion has been modified for blow up prevention. Such as the quorum sensing mechanism proposed by Hillen in (15), new formulation to a model similar to quasi-Fermi level in semiconductor modelling by Marrocco (23), modification of attractant secretion using Michaelis-Menten kinetics by Maini et. al. in (22) and by Grindrod in (5).

5.2 Reviews from The Microscopic Approach

Wolgang Alt in (1) discussed chemotaxis in stochastical models using turning frequency and turn angle distributions, and estimated error using energy functional.

Othmer et. al. in (30) gave two stochastic processes for modelling biological dispersal related to chemotaxis, by position jump process and velocity jump process.

Hillen in (17) and (12) analysed chemotaxis in hyperbolic model of one dimension by employing turning rate for individual movement patterns. In other articles (13) and (14), Hillen and Othmer studied diffusion-limit expansion of transport equation to describe the motion of individual organisms governed by Poisson process.

Coupling of kinetic model of chemotaxis to Poisson equation also was studied by Chalub et. al. (4), where it is shown that finite time blow up does not occur in the kinetic model under certain assumptions on the turning kernel.

Bibliography

[1] Wolgang Alt. Biased random walk models for chemotaxis and related diffusion approximations. *Journal of Mathematical Biology*, **9**:147–177, 1980. 5.2

[2] Michael P. Brenner and M. D. Betterton. Collapsing bacterial cylinders. *Physical Review E*, **64**:061904–1–061904–15, 2001. 3.3, 5.1

[3] Micheal P. Brenner, Peter Constantin, Leo P. Kadanoff, Alain Schenkel, and Shankar C. Venkataramani. Diffusion, attraction and collapse. *Nonlinearity*, **12**:1071–1098, 1999. 5.1

[4] Fabio A.C.C. Chalub, Peter Markowich, Benoît Perthame, and Christian Schmeiser. Kinetic models for chemotaxis and their drift-diffusion limits. Preprint, École Normale Supérieure, 2003. 5.1, 5.2

[5] Alexandra Chavez-Ross, Leah Edelstein-Keshet, Magdalena Luca, and Alex Mogilner. Chemotactic signaling, microglia, and alzheimer's disease senile plaques: Is there a connection? *Bulletin of Mathematical Biology*, **65**:693–730, 2003. 2.1, 3.1, 3.4, 5.1

[6] Leah Edelstein-Keshet. *Mathematical Models in Biology*. The Random House/Birkhäuser Mathematics Series, 1988. 3.1, 3.1, 3.2.2, 3.4

[7] Christopher P. Fall, Eric S. Marland, John M. Wagner, and John J. Tyson. *Computational Cell Biology*. Springer-Verlag, 2002. 3.1

[8] Morton E. Gurtin and Richard C. MacCamy. On the diffusion of biological populations. *Mathematical Biosciences*, **33**:35–49, 1977. 3.4

[9] Miguel A. Herrero, E. Medina, and Juan J.L. Velázquez. Self-similar blow-up for a reaction-diffusion system. *Journal of Computational and Applied Mathematics*, **97**:99–119, 1998. 3.3, 5.1

[10] Miguel A. Herrero and Juan J.L. Velázquez. Chemotactic collapse for the keller-segel model. *Journal of Mathematical Biology*, **35**:177–194, 1996. 3.3, 5.1

[11] Miguel A. Herrero and Juan J.L. Velázquez. Singularity patterns in a chemotaxis model. *Mathematische Annalen*, **306**:583–623, 1996. 3.3

[12] Thomas Hillen. Hyperbolic models for chemosensitive movement. *Mathematical Models and Methods in Applied Sciences*, **12**:1–28, 2002. 5.2

[13] Thomas Hillen and Hans G. Othmer. The diffusion limit of transport equations derived from velocity-jump processes. *SIAM Journal of Applied Mathematics*, **61**:751–775, 2000. 5.2

[14] Thomas Hillen and Hans G. Othmer. The diffusion limit of transport equations ii: Chemotaxis equations. *SIAM Journal of Applied Mathematics*, **62**:1222–1250, 2002. 5.2

[15] Thomas Hillen and K. Painter. Global existence for a parabolic chemotaxis model with prevention of overcrowding. *Advances in Applied Mathematics*, **26**:280–301, 2001. 3.1, 5.1

[16] Thomas Hillen and Kevin J. Painter. Volume-filling and quorum-sensing in models for chemosensitive movement. *Can. Appl. Math. Quart.*, **26**:280–301, 2002. (document), 2.1, 3.1, 3.4, 3.4, 3.4.1

[17] Thomas Hillen and A. Stevens. Hyperbolic models for chemotaxis in 1-d. *Nonlinear Analysis: Real World Applications*, **1**:409–433, 2000. 5.2

[18] Dirk Horstmann. From 1970 until present: The keller-segel model in chemotaxis and its consequences i. Preprint, Max-Planck-Institut für Mathematik in Leipzig, 2003. 2.2, 3.4

[19] W. Jäger and S. Luckhaus. On explosions of solutions to a system of partial differential equations modelling chemotaxis. *Transactions Of The American Mathematical Society*, **329**:819–824, 1992. 3.3

[20] Claes Johnson. *Numerical Solution of Partial Differential Equations by the Finite Element Method*. Studentlitteratur, 1987. 3.5

[21] C.C. Lin and Lee. A Segel. *Mathematics Applied to Deterministic Problems in the Natural Sciences*. SIAM, 1988. 2.2

[22] P.K. Maini, M.R. Myerscough, and K.J. Painter. Pattern formation in a generalized chemotactic model. *Bulletin of Mathematical Biology*, **60**:1–26, 1998. 5.1

[23] A. Marrocco. 2d simulation of chemotactic bacteria aggregation. Research report, Institut National De Recherche En Informatique Et En Automatique, 2002. 5.1

[24] James D. Murray. *Mathematical Biology*. Springer-Verlag, 1990. 1, 3.1

[25] James D. Murray. *Mathematical Biology Vol. II: Spatial Models and Biomedical Applications*. Springer-Verlag New York, 2003. 3.2.2

[26] Toshitaka Nagai. Global existence of solutions to a parabolic system for chemotaxis in two space dimensions. *Nonlinear Analysis, Theory, Methods and Applications*, **30**:5381–5388, 1997. 3.3

[27] Toshitaka Nagai and Takasi Senba. Behavior of radially symmetric solutions of a system related to chemotaxis. *Nonlinear Analysis, Theory, Methods and Applications*, **30**:3837–3842, 1997. 3.3, 5.1

[28] Akira Okubo. *Diffusion and Ecological Problems: Mathematical Models*. Springer-Verlag, 1980. 1, 2.3, 3.1

[29] Hans G. Othmer and Angela Stevens. Aggregation, blowup, and collapse: The abs's of taxis in reinforced random walks. *SIAM Journal of Applied Mathematics*, **57**:1044–1081, 1997. 3.4

[30] H.G. Othmer, S.R. Dunbar, and W. Alt. Models of dispersal in biological systems. *Journal of Mathematical Biology*, **26**:263–298, 1988. 5.2

[31] K. Painter, P. Maini, and H. Othmer. Stripe formation in juvenile pomacanthus explained by a generalized turing mechanism with chemotaxis. *Proceedings of the National Academy of Sciences USA*, **41**:5549–5554, 0000. 2.1

[32] Kevin J. Painter and Jonathan A. Sherratt. Modelling the movement of interacting cell populations. *Journal of Theoretical Biology*, **225**:327–339, 2003. 3.4

[33] Katharina Post. *A Non-linear Parabolic System Modeling Chemotaxis with Sensitivity Functions.* PhD thesis, Humboldt Universität zu Berlin, 1999. 3.1, 5.1

[34] Lee A. Segel. *Modeling Dynamic Phenomena in Molecular and Cellular Biology.* Cambridge University Press, 1989. 2.2, 2.2.1

[35] Peter J.M. van Haastert. Sensory adaptation of dictyostelium discoideum cells to chemotactic signals. *Journal Cell Biology*, **96**:1559–1565, 1983. 2.1

[36] Cornelis J. Weijer and Jeffrey G. Williams. Dictyostelium: Cell sorting and patterning. *Nature Encyclopedia of Life Sciences*, **10**:doi:10.1038/npg.els0001116, 2001. (document), 2.1, 2.3

Correction

- Acknowledgement:
  I would like **to thank those that** have supported me ...
- Page 20: In this equation we can see the domination of **chemotactic flux** (second term) ....
- Page 20, equation 3.49:

$$J_1 \sim \frac{-\mathbf{D_1}u + \alpha\chi u M^{2D} D_2^{-1}}{l}$$

- Page 32, equation 3.95:

$$= \int_\Omega U_{n-1} w dx + k_n \int_\Omega \chi U_n \mathbf{q}(\mathbf{U_n}) \nabla V_n \cdot \nabla w dx$$